(INVITED PAPER - International Ion Beam Engineering Congress, Sept. 12-16, 1983 in Kyoto, Japan)

IONIZATION PHENOMENA AND SOURCES OF NEGATIVE IONS

G. D. Alton

Physics Division, Oak Ridge National Laboratory*, Oak Ridge, TN 37830 USA

1. Introduction

The increasing demand for intense negative heavy ion beams for use in high energy, accelerator based atomic, nuclear and applied research, as well as low energy fundamental atomic physics and controlled thermonuclear research programs, has motivated the development of a variety of negative ion sources during the past few years. Developments such as those described in this report have been given additional impetus by the advent of large tandem accelerators under construction or in operation at various installations around the world which, in combination with other acceleration devices, have the capability of accelerating many heavy nuclei above the Coulomb barrier. These acceleration facilities will open up new avenues in high energy, heavy ion-nuclear as well as atomic physics research. Their use in tandem accelerator applications permits an increase in final beam energy and offers the great practical advantage of easy maintenance accessibility because of source operation outside the high voltage and insulating gas environment of the accelerator.

In addition to the traditional fundamental high energy research applications, a number of practical uses of negative ions have evolved over the past several years. Several examples can be cited which are illustrative of their increasing practical importance.

Negative ions are presently being used in a fast developing mass analysis technique which employs the tandem accelerator (tandem accelerator mass spectrometry). The fact that several elements do not form stably bound ground state negative ions permits the elimination of possible isobar contaminants in the mass spectra through the use of this species discrimination technique. A classic example of this technique and its experimental utilization is exemplified by the elimination of ^{14}N isobaric contamination in ^{14}C biological sample dating tandem mass spectrometry experiments [1]. The use of negative ions in this application coupled with the mass per unit charge (m/q) and energy E selectivity of the tandem accelerator permits analyses of geological and biological samples to degrees of precision unattainable with other techniques (achievable sensitivities of a few parts in 10^{16}) [2].

Negative ions are fragile entities because of their low electronic binding energies (electron affinities) and thus can be readily collisionally detached to form neutral beams. Because of the high equilibrium neutral beam fractions which can be formed in collisional detachment processes compared to those formed in positive ion collisional attachment processes, they are important as sources of neutral beams for injection into plasma fusion research devices (e.g. Refs. 3 and 4). They are being utilized in tandem accelerator based high energy ion implantation of substitutional and interstitial dopants in semiconducting materials [5], radiation damage [6,7], high energy sputtering [8], in surface analysis based on Rutherford backscattering [9], secondary ion mass spectrometry [10], x-ray fluorescence [11], depth profiling [12], and many other potential applications as exemplified by topics presented in these proceedings.

DISCLAIMER

These and other negative ion applications have provided the impetus for the development of sources capable of producing negative ion beams containing almost every element in the periodic chart. Several versions of negative ion sources which utilize the high probability processes of polar dissociative attachment and dissociative electron attachment, ternary collisional processes, charge exchange and surface ionization have been described in the literature. The species capability of a particular source may be quite limited or rather universal depending on the mechanism employed. The negative ion intensity capabilities of a particular source also depend strongly on the mechanism of generation utilized as well as the electron affinity of the species involved.

Stable Ion Formation — The Electron Affinity. The processes involved in the attachment of electrons to neutral atoms or molecules are exothermic in contrast to the endothermic processes required for positive ion formation. The binding energy or electron affinity E_A of the negative ion is a measure of the stability and ease of ion formation. The electron affinity E_A is defined as the difference between the ground state neutral E_0 and negative ion E_i energies or

$$E_A = E_0 - E_i \qquad (1.1)$$

and must be positive for ion stability. Negative values refer to unstable negative ion states.

The probability of negative ion formation depends significantly on the value of E_A as well as the method used in the formation process. Approximately 75% of the naturally occurring elements have positive electron affinities. The table below displays experimentally determined atomic electron affinities for many of the naturally occurring elements — many of which were taken from the compilations of Ref. 13. We note that Groups IIA, IIB, and VIIIA, as well as the elements N, Sc, Mn, Y, and Hf, all have negative electron affinities and thus do not form stably bound ground state negative ions.

IONIZATION POTENTIALS AND ELECTRON AFFINITIES OF THE ELEMENTS

GROUP IA							VIII A
1 H 13.595 0.7542	IIA	IIIA	IVA	VA	VIA	VIIA	2 He 24.58 0.078*
3 Li 5.39 0.620	4 Be 9.32 <0	5 B 8.30 0.28	6 C 11.26 1.268	7 N 14.54 <0	8 O 13.61 1.462	9 F 17.42 3.399	10 Ne 21.56 <0
11 Na 5.14 0.548	12 Mg 7.64 <0	13 Al 5.98 0.46	14 Si 8.15 1.385	15 P 10.55 0.743	16 S 10.36 2.0772	17 Cl 13.01 3.615	18 Ar 15.76 <0
19 K 4.34 0.5012	20 Ca 6.11 <0	31 Ga 6.00 0.3	32 Ge 7.88 1.2	33 As 9.81 0.80	34 Se 9.75 2.0208	35 Br 11.84 3.364	36 Kr 14.00 <0
37 Rb 4.18 0.4860	38 Sr 5.69 <0	49 In 5.78 0.3	50 Sn 7.34 1.25	51 Sb 8.64 1.08	52 Te 9.01 1.9708	53 I 10.46 3.061	54 Xe 12.13 <0
55 Cs 3.89 0.4715	56 Ba 5.21 <0	81 Tl 6.11 0.3	82 Pb 7.41 1.1	83 Bi 7.28 1.1	84 Po 8.43 1.9	85 At 9.5 2.8	86 Rn 10.74 <0

IIIB	IVB	VB	VIB	VIIB	VIII B			IB	IIB
21 Sc 6.56 <0	22 Ti 6.83 0.2	23 V 6.74 0.5	24 Cr 6.76 0.66	25 Mn 7.43 <0	26 Fe 7.90 0.25	27 Co 7.86 0.7	28 Ni 7.63 1.15	29 Cu 7.72 1.226	30 Zn 9.38 <0
39 Y 6.5 =0	40 Zr 6.96 0.5	41 Nb 6.77 1.0	42 Mo 7.18 1.0	43 Tc 7.28 0.7	44 Ru 7.38 1.1	45 Rh 7.46 1.2	46 Pd 8.33 0.6	47 Ag 7.57 1.303	48 Cd 8.99 <0
57 La 5.61 0.5	72 Hf 7. <0	73 Ta 7.88 0.6	74 W 7.98 0.6	75 Re 7.87 0.15	76 Os 8.7 1.1	77 Ir 9. 1.6	78 Pt 8.96 2.128	79 Au 9.22 2.3088	80 Hg 10.43 <0

*METASTABLE

In addition to negative atomic species formation, many molecular negative ions have been observed. Such ions are of considerable importance to tandem Van de Graaff accelerator users who often must rely on molecular negative ion formation in order to meet the species and intensity requirements of particular experiments. In many cases, molecular negative ions containing the element of interest have much higher electron affinities and therefore can be formed with higher probability than can the atomic species. In fact, molecular ions may offer the only alternative of producing beams containing elements which do not form stably bound negative ion states. The unwanted species can be easily rejected by collisional

dissociation in the positive ion formation process (stripping) followed by magnetic (m/q) analysis. However, due to the partition of energy among the molecular ion constituents, the first stage of acceleration before stripping results in a lower energy for the desired species.

Metastable Negative Ion Formation. There is an important class of negative ions which are formed in excited states of the parent atom and live long enough to be of use experimentally. Such longlived states are categorized as being metastable. In order to induce electron attachment and thus form such states, it is necessary, first of all, to form a particular excited electronic state of the neutral atom to which an electron can be attached. The subsequently formed negative ion may live for extended periods of time if the excited compound state is forbidden to decay.

A classic example of a metastable negative ion which can only be formed through attachment to an excited state of the atom is that of He^-. These ions form with high probability in the $He^-(^4P)$ state as a result of sequential collisions with low ionization potential charge exchange vapors according to the following reactions

$$He^+ + M^0 \rightarrow He^{0*} + M^+$$

$$He^{0*} + M^0 \rightarrow He^{-*} + M^+. \qquad (1.2)$$

The attachment energy is 0.078 eV relative to the $He^{0*}(^3S)$ state and is metastable against spin-spin interactions. The lifetime of the negative ion depends on the particular magnetic substate; the $P_{1/2,3/2}$ states have lifetimes of ~10 and 16 μsec, respectively, and the $P_{5/2}$ substate has a much longer lifetime (~500 μsec) [14,15].

Several other metastable ions also have either been observed experimentally or theoretically predicted, including members of the Group IIA elements which are thought to have negative electron affinities (e.g. Be^-, Ca^-). In contrast to He^-, very little information is available concerning the binding energies and states of formation or lifetimes of other metastable ions. However, Be^- and Ca^- have been generated and used experimentally in accelerator applications and therefore must have lifetimes of the order of a few μsec [16,17].

Reviews exclusively devoted to the subject of negative ion sources have been previously given by Dawton [18] and Middleton [19] while brief inclusions of the subject have been contained in more general ion source review articles [20,21]. In the present review, limited discussions will be made of the elementary physical processes which underlie negative ion formation. The major types of negative ion sources and their principles of operation will also be described. Examples of sources will be presented which are based on a particular or combination of ion generation mechanisms. Because of the requirement of brevity and the many variations of ion sources based on a particular principle, it will be impossible to reference all reported sources and their performance characteristics. For these reasons, many sources such as the large multiple aperture devices used in plasma fusion reactor injectors will not be emphasized. As well, methods of spin polarization and their associated sources will not be included. The reader is referred to the literature for discussions of these and related subjects.

Negative ions may be formed by means of several physical or physiochemical processes including radiative capture, dielectronic recombination, polar dissociation, dissociative attachment, ternary collisional processes, charge exchange and by thermodynamic equilibrium and non-thermodynamic equilibrium surface ionization.

2. Negative Ion Formation Through Electron Impact

A large number of sources, described categorically as direct extraction plasma sources, produce ions in dilute or high density plasma media in which the following generation mechanisms are believed to be operative. For further discussions of the following processes, the reader is referred to the text by Massey [22].

Radiative Capture. The simplest way in which negative ions can be formed is by direct capture of a free electron by a neutral atom. For attachment to take place, the initial kinetic energy of the electron T_e plus the electron affinity E_A must be released through radiation or transfer to a third body. Such mechanisms are referred to as radiative capture processes and are characterized by a continuum emission of radiation with longest wavelength given by

$$\lambda = \frac{hc}{E_A} \tag{2.1}$$

whenever third body energy transfer processes are not involved. The process, however, occurs with low probability and, therefore, is not a practical means of producing negative ions.

Dielectronic Attachment. Another attachment mechanism is possible involving radiative stabilization. Attachment is possible if the incident electron has energy such that the energy of the atom plus electron is within the level width of a doubly excited state of the atom. Thus, it is possible to capture the electron in certain allowed states without emission of radiation. Once formed the ion may revert to the ground state by radiative emission or revert to the neutral by ejecting the electron back into the continuum. Dielectronic attachment is also a low probability process and therefore not important in high intensity negative ion sources.

Polar Dissociative Attachment. Attachment may occur as a result of photon or electron as well as other heavy particle interactions with molecular neutrals in which sufficient energy is imparted to the molecule to excite the molecule to an unstable state which dissociates spontaneously into positive and negative ions.

Polar photodissociative attachment is a process whereby a molecule xy absorbs a photon of sufficient energy hν to cause spontaneous fragmentation according to the reaction

$$xy + h\nu \rightarrow x^- + y^+ \tag{2.2}$$

Negative ion formation may also occur by this mechanism, as well, whenever an electron of sufficient energy for molecular excitation to an unstable state interacts with a molecule xy as follows

$$e + xy \rightarrow x^+ + y^- + e. \tag{2.3}$$

We note that the electron is not itself captured but only serves as the means by which the molecular excitation occurs.

In polar dissociation processes the Franck-Condon principle [23,24] can be involked to estimate the relative kinetic energy of the x^+ and y^- ions after the collision. If the minimum energy transfer necessary for molecular fragmentation to occur is given by E_{min} and the dissociation energy D_{xy} is known along with the ionization energies of the positive and negative ion fragments E_i, E_A respectively, the minimum relative kinetic energy T of the fragments can be calculated from the following expression:

$$T = E_{min} + E_A - E_i - D_{xy}. \tag{2.4}$$

The process is illustrated in Fig. 1 which displays the potential energy curves associated with the polar dissociation process. Since low ion energy spreads are desirable for ion source applications, a knowledge of the respective potential energy curves is useful in predicting energy spreads in ion sources which utilize this principle.

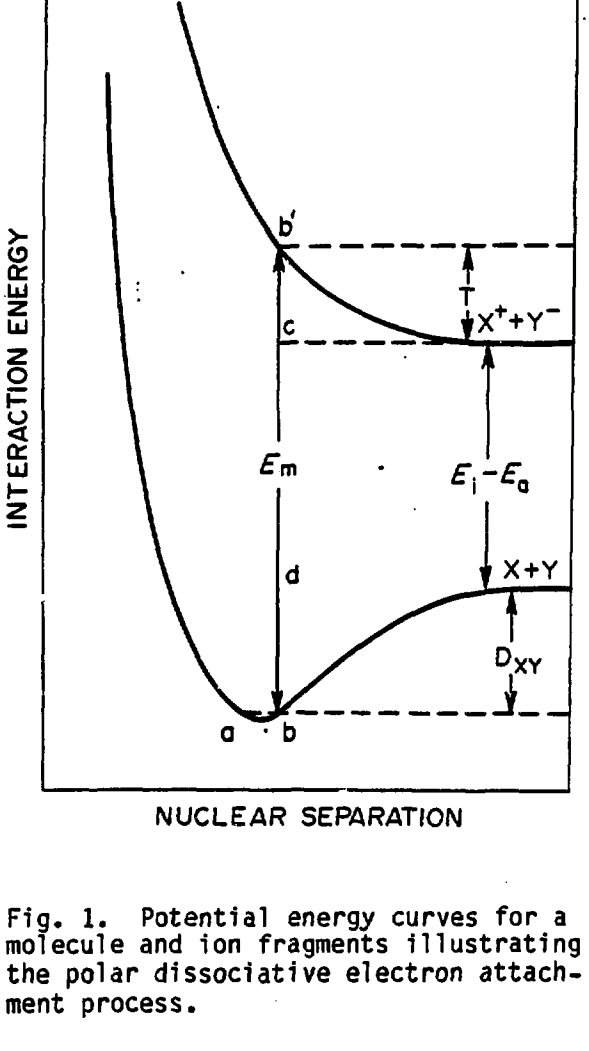

Fig. 1. Potential energy curves for a molecule and ion fragments illustrating the polar dissociative electron attachment process.

Dissociative Attachment. Electrons may be stably attached to atoms during their interactions with molecular neutrals according to the following reactions

$$e + xy \rightarrow x^- + y$$

$$e + xy \rightarrow x + y^-. \tag{2.5}$$

The process may be viewed as a three-body process where the excess energy released during the reaction can be adsorbed by transfer to the relative motion of the atomic nuclei or fragments and thus the state can be readily stabilized. Such processes are characterized by curve crossing of the respective molecular-neutral and negative-neutral potential energy curves as illustrated in Fig. 2.

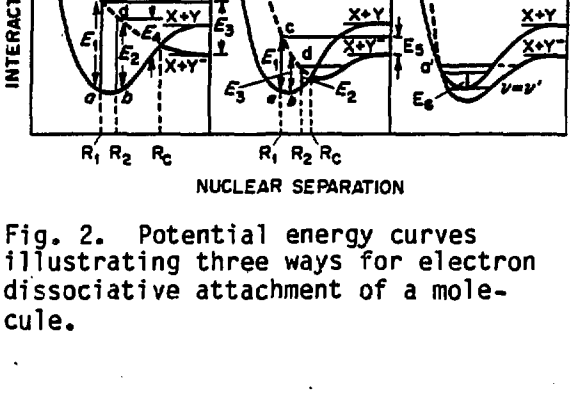

Fig. 2. Potential energy curves illustrating three ways for electron dissociative attachment of a molecule.

In Figs. 2a, b, and c, the solid curves refer to the ground or normal states of the neutral molecule xy; the dotted curves refer to states of the molecular negative ion. In the limit toward infinite nuclear separation, the curves are spread apart by an amount equal to the electron affinity of the atom y. The range of nuclear separations $R_1 \rightarrow R_2$ corresponds to the amplitude of oscillation (a → b) of the molecule in the ground or normal state. The transition resulting in electron capture will occur at points c and d, provided that the nuclear coordinates R_1 and R_2 remain fixed (Franck-Condon principle). Autodetachment can occur over a considerable range of nuclear separations. Molecules which survive without autodetachment will dissociate into an atom x and an ion y^- with relation kinetic energy between E_3 and E_4. Once the nuclear separation R passes R_c, autodetachment can no longer take place (Fig. 2a).

In Fig. 2b, electrons captured with energy between E_3 and E_1 can produce dissociative attachment of atoms x and ions y^- with relative energies between 0 and E_5. Electrons which are captured with energies E_2 and E_3 induce vibrational excitation of the molecule xy^-.

Attachment to the molecule can occur for molecules with positive electron affinities without dissociation thereby forming the molecule xy^-. Vibrational states of the molecule will be stable for frequencies $\nu < \nu'$; those with vibrational frequencies $\nu > \nu'$ will be unstable toward autodetachment (Fig. 2c). Again this process is possible because electronic excitations take place on a time scale short with respect to the motion of nuclei (Franck-Condon principle).

Production through Ternary Collisions between Electrons and Molecules. Ternary collisions are the most efficient in producing negative ions in a dense gas at low electron energies. These occur as follows:

$$\begin{aligned} e + A + B &\rightarrow A^- + B \\ A + 2e &\rightarrow A^- + e \end{aligned} \qquad (2.6)$$

where A,B are atoms or molecules, and e is the electron. The first process is of much greater practical importance because the second occurs only in systems with high electron densities.

While all of the previously discussed radiative and collisional processes may take place in certain types of negative ion sources, radiative and dielectronic capture are known to be low probability processes and, therefore, are not practical mechanisms for negative ion production. In most sources utilizing charged particles for production (electrons or ions) photo-polar dissociation processes are infrequent because of the low photon flux environment. In direct extraction plasma type sources, electron polar dissociation, dissociative attachment, and three-body (ternary) collisional transfer processes dominate.

Although plasma type sources were initially developed for positive ion generation, they can be utilized as negative ion sources by simply reversing the ion extraction polarity. Several reviews have been made of the properties of positive plasma type sources including those described in Ref. 25.

2.1 Types of Electron Impact Attachment Sources.

Sources which employ electron impact ionization methods from which negative ions can be extracted are often referred to as direct extraction type sources. Almost all sources of this type produce ions by means of electron

attachment in the atmosphere of a plasma. These sources characteristically have lower emittances than sources which utilize charge exchange or sputtering to produce negative ions. Many sources have been described in the literature among which the following serve as examples:

Duoplasmatron Sources. The duoplasmatron ion source, described by Von Ardenne [26] is widely used at accelerator installations, primarily for the production of ion beams from noncorrosive gaseous materials. A discharge is maintained between a hot cathode and an anode. A strong inhomogeneous magnetic field (3-10 kG) maintained between an intermediate electrode and the anode concentrates the discharge near the extraction aperture in the anode region. The plasma in the anode region attains densities of the order of $n_e \cong 1 \times 10^{14}$ from which ions beams are extracted. A schematic drawing of the plasma and extraction regions of the source is shown in Fig. 3.

Moak et al. [27] first discovered that useful intensities of negative ions could be directly extracted from a duoplasmatron operated with reversed extraction polarity. Later it was discovered that the negative ions were more abundant in the periphery of the plasma and the yield of negative ions could be increased by off setting the extraction electrode with respect to the plasma center [28].

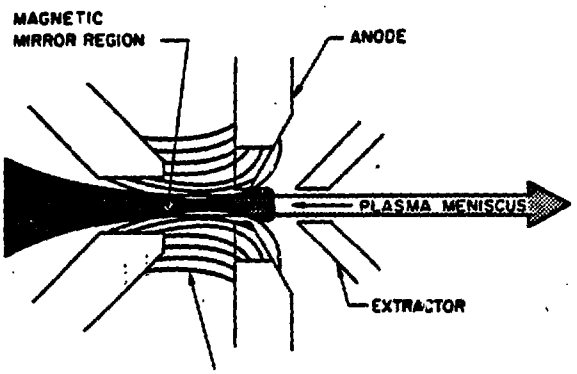

Fig. 3. Schematic drawing of the plasma and ion extraction region of the duoplasmatron ion source.

A direct extraction hollow cathode duoplasmatron H^- ion source has been described by Kobayashi, Prelec and Sluyters which generates H^- ion currents up to 60 mA in the pulsed extraction mode [29]. The maximum intensity is found to be on axis due to the lower plasma density at the center of the hollow cathode and, therefore, there is no need to offset the extraction electrode as with the conventional duoplasmatron.

The duodecatron [30] and triplasmatron [31] versions of the duoplasmatron have been developed which permit the use of corrosive gaseous materials which could otherwise affect the lifetime and stability of operation of the conventional duoplasmatron.

The duodecatron version uses a hollow cathode instead of a heated filament to sustain the arc discharge. Differential isolation is effected by an aperture placed between the primary discharge and the intermediate electrode which allows gases containing the element of interest to be introduced in the intermediate electrode-anode region where negative ions are extracted.

The triplasmatron version allows the plasma from the intermediate electrode-anode region to expand into a positive biased expansion cup into which a gaseous compound or elemental material is introduced. Negative ions then are extracted from an aperture in the expansion cup. The duodecatron version has produced currents of over 100 μA H^-; and 10 μA or greater of O^-,

F^- and Cl^-. Currents of O^- in excess of 50 μA have been extracted from the triplasmatron ion source.

The Diode Source. Many other direct extraction sources have been developed for production of negative ion beams including the diode source of Bastide et al. [32]. The diode source has been used to generate several negative ion species. Among those reported are 600 μA H^-; 20 μA BO^-; 0.5 μA C^-; 10 μA CN^-; 4 μA O^-; 50 μA F^-; 4 μA P^-; and 4 μA S^-.

Penning Discharge Sources. The Penning discharge ion source consists of two cathodes placed at the ends of a cylindrical hollow anode. Electrons, produced in the discharge, oscillate between the cathodes and are constrained from moving to the anode cylinder by means of magnetic field directed parallel to the axis of the anode. Versions of the source exist for which ion extraction is made through an aperture in the end of the cathode (end extraction) or through an aperture in the anode (side or radial extraction). The latter geometry is compatible with slit apertures. Some sources employ hot cathodes which emit electrons thermionically to initiate the discharge while others use cold cathodes where electrons are emitted principally by secondary processes. The cathode, in the hot cathode version, may be directly or indirectly heated.

Both radial and axial Penning discharge sources have been utilized for negative ion generation. The radial configuration, in general, produces higher negative ion yields due to the more diffuse region of the plasma from which the ions are extracted. High density plasmas tend to deplete the negative ion component due to collisional processes. The radial extraction geometry Penning source of Heinicke et al. [33] is shown in Fig. 4. The material to be ionized may be introduced into the discharge as a gas, directly vaporized from an oven, or sublimed from a solid rod of the material. A variety of negative ion species have been extracted from the source including 1.2 μA Li^-; 60 μA H^-; 0.2 μA BeH^-; 1.0 μA MgH^-; 100 μA F^-; 10 μA B^-; 50 μA S^-; and 50 μA Cl^-.

Another direct extraction radial geometry Penning ion source, shown in Fig. 5, has been described by Smith and Richards [34]. The source utilizes sputtering from the cathodes to generate neutral vapor of the desired species while introducing cesium vapor into the discharge chamber. The addition of cesium in the discharge greatly increases the probability of negative ion formation. Beam intensities of 2.7 μA C^-; 6.5 μA Cu^-; 4 μA Ni^- have been reported.

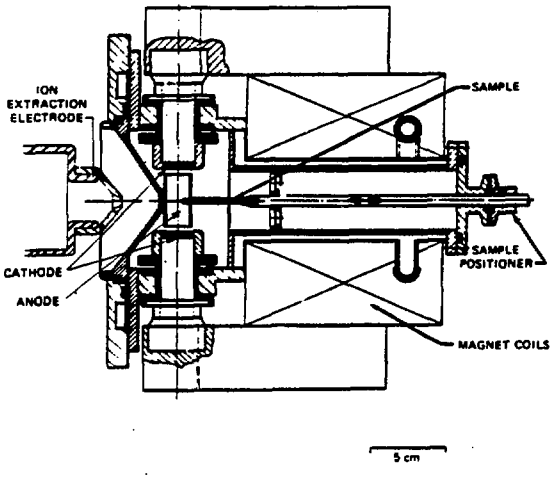

Fig. 4. Schematic drawing of a direct-extraction radial-Penning-discharge negative ion source [Ref. 33].

The performance characteristics of a multiple aperture, axial geometry Penning source which operates in a cesium rich plasma mode has been described by Prelec [35]. The source was designed for production of high intensity beams of H^- for possible use in neutral beam fusion research reactor devices.

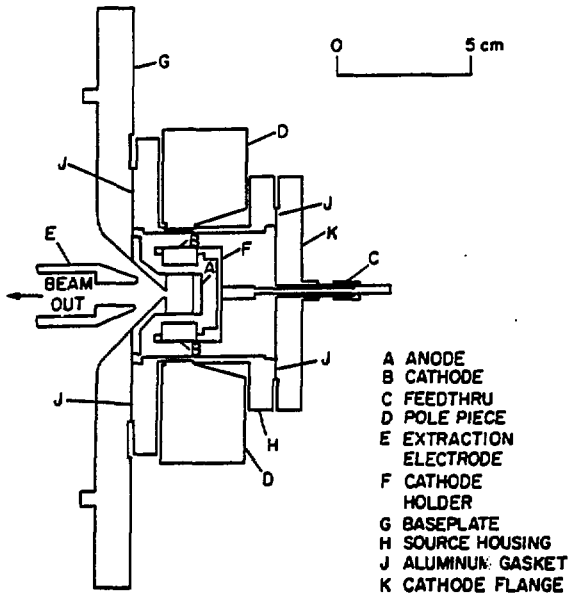

Fig. 5. Schematic drawing of a direct-extraction radial-Penning-discharge negative ion source [Ref. 34].

3. Negative Ion Formation Through Charge Exchange

The electron-capture and loss processes which take place during collisions between energetic ions and atoms or molecules in a gaseous vapor result in a statistical distribution of charge states of the emergent beam. Equilibrium between the competing capture and loss processes takes place whenever the beam passes through a target of sufficient thickness. A particular emergent charge state is in equilibrium whenever the fraction no longer depends on further increases in target density. For example, the differential equation which relates the dependence of the fractional yield F_- for formation of H^- through charge exchange in a vapor of thickness π is given by

$$dF_-/d\pi = \sigma_{+-} F_+ + \sigma_{0-} F_0 - (\sigma_{-+} + \sigma_{-0})F_- \qquad (3.1)$$

where σ_{+-}, σ_{0+}, σ_{-+}, σ_{-0} are, respectively, the cross sections for conversion of the positive to a negative ion, from a neutral atom to a negative ion, from a negative to a positive ion, and from a negative ion to a neutral atom. Negative ion conversion from an initially positive ion beam interacting with a low ionization potential vapor can take place with high probability. The mechanism is therefore a very practical method for the production of negative ion beams and has been utilized for this purpose for several years. According to the experimental measurements of Donally and Thoeming in the production of He^- in Cs exchange vapors [36], the electron transfer process takes place in sequential collisions according to the following reactions

$$y^+ + x \rightarrow y^{0*} + x^+$$
$$y^{0*} + x \rightarrow y^{*-} + x^+. \qquad (3.2)$$

Production efficiencies depend primarily on ion energy, the electron affinity of the element under consideration, as well as the electron binding energy of the donor material. For efficient ion production, members of the Groups IA and IIA elements are usually utilized.

Several other investigations have been made of the probabilities and energy dependencies of charge exchange formation of H^- in Na [37], and Cs vapors [38] and He^- in Li, Na and Mg [39], K [40], Rb [41], and Cs [42] vapors.

Extensive and systematic investigations of the exchange production of many ions in sodium and magnesium vapors have been reported in recent years [43,44]. These investigations show that production efficiencies ranging from ~0.5 to >90% for the elements considered. Equilibrium fractions as a function of ion energy for several ions in the exchange vapors of Na and Mg are illustrated in Figs. 6 and 7. These studies show that Mg is a more effective electron donor for high electron affinity elements while Na vapor is desirable for the production of beams from low affinity materials.

As pointed out previously, this mechanism offers a practical and efficient means of producing useful beams from elements which have negative electron affinities. Many of these ions can be formed in metastable excited states with relatively high efficiencies so that they can be used in accelerator based experimental studies.

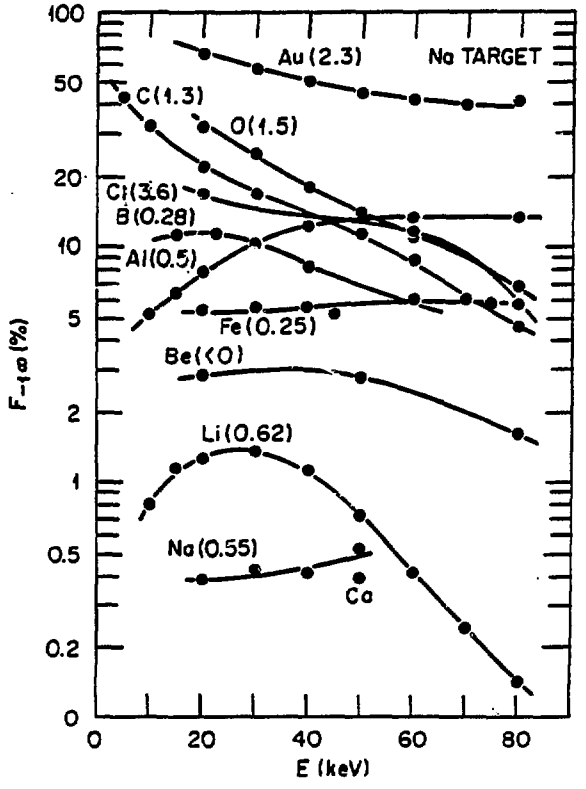

Fig. 6. Negative ion equilibrium charge exchange fractions versus ion energy for several ions in sodium exchange vapor [Ref. 43].

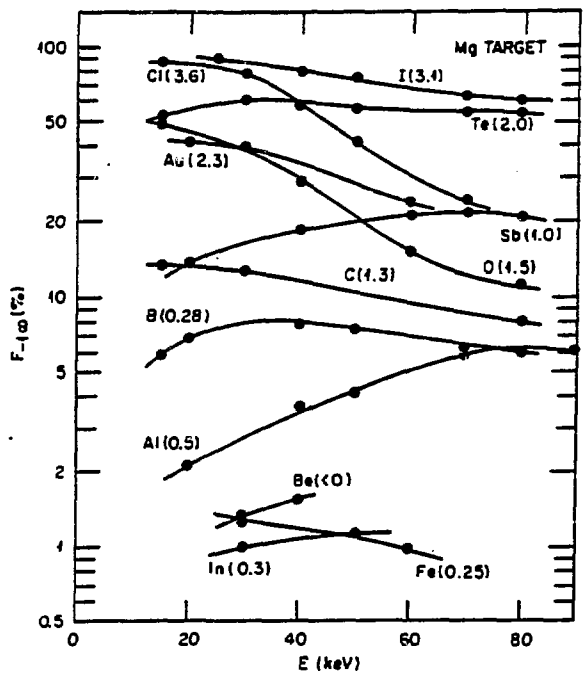

Fig. 7. Negative ion equilibrium charge exchange fractions versus ion energy for several ions in magnesium exchange vapor [Ref. 44].

3.1 Types of Charge Exchange Sources

Several exchange type negative ion sources have been described in the literature. The source consists of a positive ion source (usually a duoplasmatron or radiofrequency source) and a charge exchange canal where the exchange interactions take place. The exchange canal is usually a tube ~0.75 cm in diameter and ~5 cm in length to which is attached a gas line or an oven for introducing the gaseous or solid exchange vapors. In the case of the use of solid materials, the temperature of the oven and canal can be controlled rather precisely. The canal region can be biased negative with respect to the source at ground potential or the source can be biased positive with respect to the canal at ground potential (bias potentials of 10 → 40 keV are usually employed). The former configuration permits extraction of negative ions which are generated by the positive ion beam from the exchange vapor itself [45]. In this particular, mode of operation, the formation processes are not through exchange but polar dissociation, dissociative attachment and ternary collisional processes. An einzel lens is usually placed between the positive ion source and the canal for focusing the positive ion beam through the small diameter canal.

A schematic of a duoplasmatron charge exchange source is shown in Fig. 8 [46]. The exchange canal in this source is biased negative relative to the grounded positive source to enable extraction of negative ions generated from the exchange vapor itself.

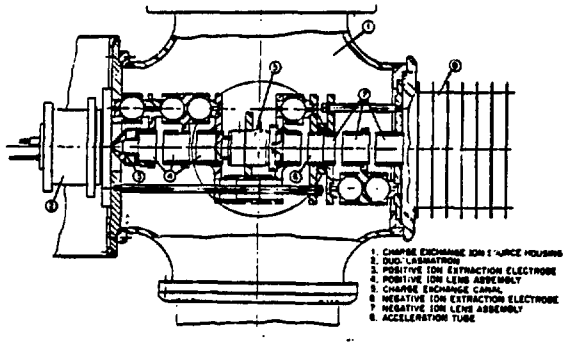

Fig. 8 Schematic diagram of a duoplasmatron charge exchange source [Ref. 46].

Considerable efforts have been expended toward development of high intensity negative ion sources for the production of H^- and He^- for use in neutral particle injectors for fusion energy research. The charge exchange technique has been utilized by Hooper et al. [47] in the production of >70 mA of He^- through exchange with Na vapor. The positive ion beam was generated in a large multiple aperture source which was operated in a pulsed mode.

Gaseous feed type positive sources, usually utilized, (duoplasmatrons or radiofrequency type sources) restrict the number of species that can be generated in this type of negative ion source. Incorporation of a universal type positive ion source permits generation of negative ions from any element which has a positive electron affinity as well as a number of metastable ions. This universal source concept is illustrated schematically in Fig. 9 [Ref. 48]. This source employs a hollow cathode type positive ion source and a recirculating type lithium charge exchange canal developed for use in high intensity He^- ion sources [49]. Among the ion beams that such sources have been used to generate are the following: 10 μA H^-; 12 μA He^-; 1.5 μA Li^-; 2 μA C^-; 15 μA O^-; 25 μA F^-; 0.4 μA Na; 15 μA Cl^-; 1 μA S^-; 0.2 μA K^-, 10 μA I^-; and 10 μA Br^-.

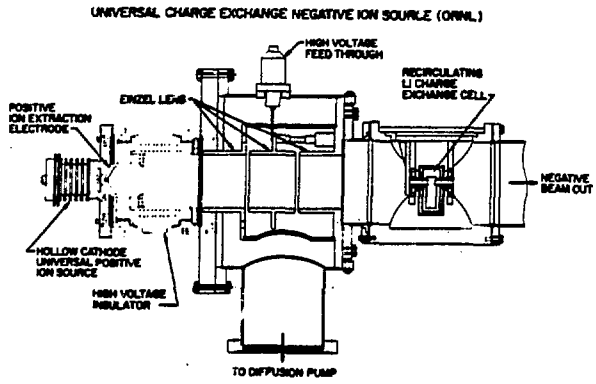

Fig. 9. Schematic diagram of a universal charge exchange source [Ref. 48].

4. Negative Surface Ionization Phenomena

Adsorption Phenomena. Electropositive atomic surface adsorption phenomena have been continually studied since the classic experiments of Taylor and Langmuir [50], Becker [51], and in more recent years by many others such as those exemplified in Refs. 52, 53 and 54. Such studies have provided fundamental information about adsorption processes and in recent years have had practical significance in terms of thermionic energy conversion and ion propulsion. Although the magnitudes of surface work function change due to electropositive or electronegative atom adsorption are difficult to theoretically quantify, the basic mechanisms responsible have long been understood. Many emission phenomena, such as thermionic, field, photoelectric, and surface ionization processes, depend directly on the value of the surface work function. The magnitude and sign of the effected change during adsorption depends on the chemical properties of the adsorbed atom (adsorbate) and those of the host material (adsorbant).

The influence of adsorption of positive or negative ions on the work function of an adsorbant can be readily seen by applying simple electrostatic theory to compute changes in energy required to transfer an electron from the metal into the vacuum region. This simple The physical picture is qualitatively correct, but the derived mathematical relationship

$$\Delta\phi = \pm 4\pi\, Ne^2\, d = \pm 4\pi\, Ne\, \mu_0 \qquad (4.1)$$

cannot be used for quantitative estimates of $\Delta\phi$ because the number density of adsorbed atoms N and $\mu = ed$, the dipole moment resulting from the electrostatic double layer, are, in general, unknown. (The value of μ changes with increasing N due to electrostatic repulsive interactions between the adsorbed ions.) In the simple picture the adsorbed alkali atoms lose their valence electrons to the substrate. The resulting positive ions induce images in the

substrate, producing dipoles which lower the work function by an amount proportional to μN, with μ the magnitude of the dipole moment per adatom, and N the number of adatoms per unit area. Each dipole, however, is depolarized by the electric field due to all the others: The greater the coverage, the greater the depolarization. The minimum in the work-function-vs-coverage curve occurs when the relative decrease in dipole moment per adatom ($d\mu/\mu$) balances the relative increase in the number of dipoles (dN/N). The picture, while conceptually useful, is not satisfactory in a detailed way. The alkali atoms are not completely ionized, the image approximation breaks down at very short distances, and it is difficult to assign a polarizability to the dipole.

A principal objective of many adsorption studies (theoretical as well as experimental) is the determination of the change in work function $\Delta\phi$ as a function of the number of atoms adsorbed per unit area N or the fractional coverage θ_c, where $\Delta\phi = \phi - \phi_0$ is the difference between the intrinsic work function θ_0 and ϕ the work function corresponding to a particular coverage N or fractional coverage θ_c. The behavior of ϕ as a function of fractional coverage θ_c for K absorbate atoms on single crystal Ta is typified by the measurements of Blaszcyzyszyn [54] shown in Fig. 10. Characteristically, the work function changes very rapidly at low fractional coverages, reaches a minimum and finally approaches a constant value equivalent to the work function of the absorbate as $\theta_c \to 1$. The minimum work function generally is observed to occur at $\theta_c \approx 0.6$ (e.g. Refs. 52 and 53).

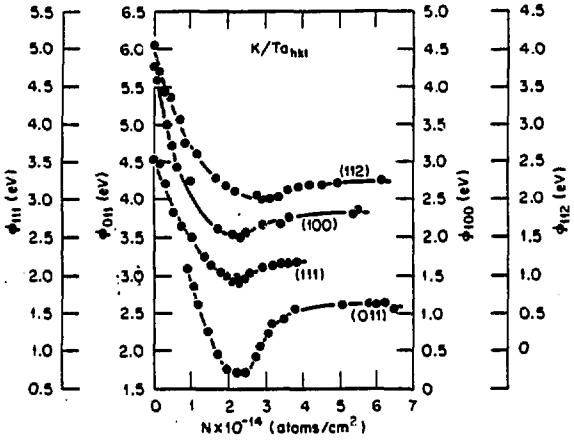

Fig. 10. Illustration of the effect of electropositive atom adsorption on the work function ϕ of single crystal Ta as a function of fractional surface coverage, θ_c [Ref. 54].

Estimation of Maximum Work Function Changes $\Delta\phi$ Due to Adsorption. Quantitative correction between theory and experiment has been seriously impeded by the lack of accurate theoretical or semiempirical analytical expressions for relating changes in work function to surface coverage. Several semiempirical relations have been proposed such as those of Miller [55] and Broeder et al. [56].

Alton and Blazey [57] used the Broeder et al. relation as the basis for developing an approximate relation for computing maximum work function changes $\Delta\phi$ which occur at optimum fractional coverages θ_c. An empirical relation was found to reproduce with good accuracy maximum work function changes for alkali and alkaline earth metal adsorption. The expression is

$$\Delta\phi(\text{eV}) \approx -1.24\ \{\phi_0 - 1/2(I_a + E_a)\}. \qquad (4.2)$$

where ϕ_0 is the intrinsic work function of the metal and I_a, E_a are respectively the ionization potential and electron affinity of the adsorbate.

Changes in work function due to adsorption of electropositive ions on high work function materials have been theoretically studied by Lang [58] by employing a simple model of the metallic substrate-adsorbate system.

4.1 Thermodynamic Equilibrium Surface Ionization

Atoms or molecules impinging on a hot metal surface may be emitted as positive or negative ions in subsequent evaporation processes after a mean residence time τ_a and τ_i. The process of direct surface ionization is statistical in nature and therefore, statistical and thermodynamic arguments can be applied to such systems to derive equations for the degrees of positive or negative ion generation under thermodynamic equilibrium conditions. The subject has been reviewed in a rather comprehensive manner by Kaminsky [59] which contains many older review references on the subject.

Consider the potential energy of an atom as a function of distance from the surface of a metal as illustrated in Fig. 11. The energy ΔHa corresponds to that required to disassociate the adsorbed atom from the metal surface. If we supply, by some means, enough energy to ionize the atom, transferring the electron from the metal to the atom in the case of electronegative atom adsorption in the process, then the atomic and ionic potential curves are separated, respectively, by the amount $\phi - E_A$, where E_A is the electron affinity of the electronegative atom and ϕ is the work function of the surface. The energy required for removing an ion from the surface is ΔHi and the condition for residing on the surface as an ion is $\Delta Hi - \phi + E_A > \Delta Ha$. An ion supplied with energy ΔHi may be transferred to the continuum either in ionic or atomic form in cases where the respective potential energy curves cross. The probability for arrival at a position far from the metal in a given state depends on the magnitude of $\phi - E_A$. For thermodynamic equilibrium processes, the ratio of ions to neutrals which leave an ideal surface can be predicted from Langmuir-Saha surface ionization theory.

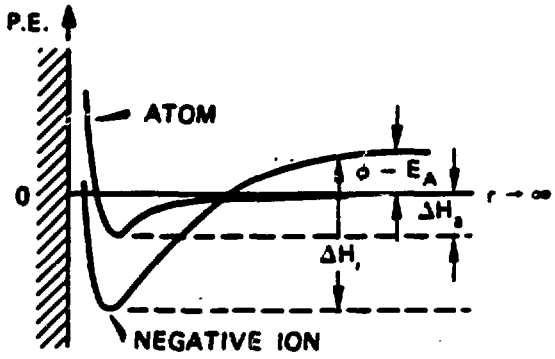

Fig. 11. Potential energy curves for an electronegative atom and ion as a function of distance from a hot metal surface.

The analogous form of the Saha-Langmuir equation for the probability of negative ion formation for neutral particles of electron affinity E_A interacting with a hot metal surface at temperature T and constant work function ϕ is

$$P_I = \frac{\frac{\omega_-}{\omega_0}\left(\frac{1 - r_-}{1 - r_0}\right) \exp(E_A - \phi)/kT}{1 + \frac{\omega_-}{\omega_0}\left(\frac{1-r_-}{1-r_0}\right) \exp(E_A - \phi)/kT} \tag{4.1.1}$$

where r^-, r_0 are the reflection coefficients of the particle at the surface and ω^-, ω_0 are statistical weighting factors for the negative and neutral ion, respectively. ω^-, ω_0 are related to the total spin of the respective ion, neutral given by

$$\omega = 2 \sum_i s + 1 \tag{4.1.2}$$

where s is the spin of the electron. If the process takes place in the presence of an electrostatic field ε, then the possibility of negative ion formation is enhanced by means of the Schottky effect provided the electric field is in a direction so as to remove the negative ions as they are formed. Expression (4.1.1) takes the following form

$$P_I = \frac{\frac{\omega_-}{\omega_0}\left(\frac{1 - r_-}{1 - r_0}\right) \exp\left[E_A + \left(\frac{q\varepsilon}{4\pi\varepsilon_0}\right)^{1/2} - \phi\right] \Big/ kT}{1 + \frac{\omega_-}{\omega_0}\left(\frac{1 - r_-}{1 - r_0}\right) \exp\left[E_A + \left(\frac{q\varepsilon}{4\pi\varepsilon_0}\right)^{1/2} - \phi\right]/kT} \tag{4.1.3}$$

where ε_0 is the permittivity of free space. Expressions (4.1.1) and (4.1.3) are more complex in reality because of the variation of ϕ with crystalline orientation in cases where the metal is polycrystalline or the surface has uniformly or non-uniformly distributed surface contaminants. All of these effects can be taken into account by appropriately summing over the admixtures of existing work functions and statistical weighting factors in the respective expressions. From the relationships it is evident that negative ion yields could be enhanced by lowering the work function ϕ, extracting in a high electric field ε or by increasing the surface temperature T for elements where $E_A < \phi$. Practical limitations imposed by the requirement of operational stability usually limit electric field strengths to values $\sim 10^4$ volts/cm or a lowering of the work function by ~0.038 eV. The greatest effect can be obtained in practice by effecting changes in the work function ϕ or increasing the surface temperature T. The former can be effected by surface adsorption of minute amounts of low work function materials such as the Group 1A and 11A elements.

4.1.1 Types of Thermodynamic Equilibrium Negative Ion Sources

Although the phenomenon of positive thermodynamic equilibrium surface ionization has been utilized for many years and a number of ion sources developed, negative surface ionization has not been utilized as frequently — principally due to the lack of chemically stable low work function materials.

A few examples, however, can be cited including the resistive heating of U [60,61] and C [62,63] to produce μA beams of UF_6^-. Several surface plasma type sources described in Section 4.2 utilize LaB_6 cathodes as converters to effect H^- ionization from backscattered H^+ ions extracted from the plasma. The material has a work function of 2.6 eV and hence can be utilized to effect efficient ionization of high electron affinity materials.

A source based on the use of LaB_6 has been described by Kashihira, Vieteke and Zellermann [64]. The source, shown schematically in Fig. 12, utilizes a porous graphite ionizer which is imprenated with LaB_6. A compound containing one of the halides is diffused through the low work function surface where it is ionized with a high degree of efficiency.

4.2 Non-thermodynamic Equilibrium Atom-Surface Interaction Phenomena

The processes for which the Saha-Langmuir relation apply are those which take place under thermodynamic or quasi-thermodynamic equilibrium. Such conditions are achievable for neutral particles incident on a surface at thermal energies where the sticking probabilities are approximately unity and consequently the residence time τ is long enough to approach thermodynamic equilibrium before evaporation occurs. However, the interactions involved in sputtering and ion scattering are not thermodynamic in nature and theories other than that of Langmuir-Saha are required for proper description.

Correlation of Negative Ion Yields with Surface Work Function. The importance of surface adsorbates on negative ion formation processes has been realized since the discovery by Krohn that negative ion yields can be greatly enhanced by sputtering a material in the presence of an alkali metal [65]. The dependence of yield on alkali metal coverage was first demonstrated by Abdullayeva et al. [66]. The first direct correlation between negative ion yield and surface work function was made recently by Yu [67]. In a systematic experimental study of the negative ion formation process Yu was able to simultaneously measure the dependence of Mo^- yield and work function change $\Delta\phi$ on cesium adsorbate coverage while bombarding clean Mo with a Ne^+ ion beam. The results of this study are shown in Fig. 13. These data reflect the importance of a very low work function surface for optimum negative ion generation. Negative ion yields from the Middleton-Adams [68] and University of Aarhus [69] type sources also exhibit maxima in the yield versus cesium coverage data.

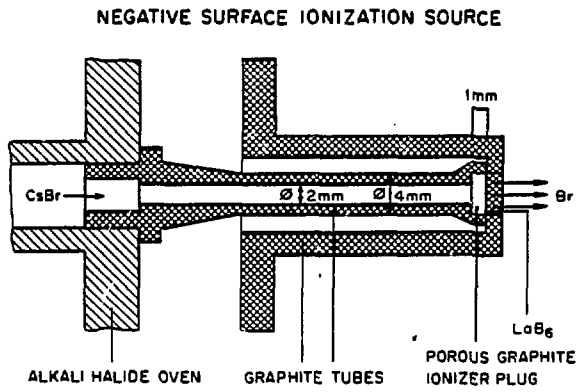

Fig. 12. Schematic diagram of thermodynamic equilibrium type negative ion source [64].

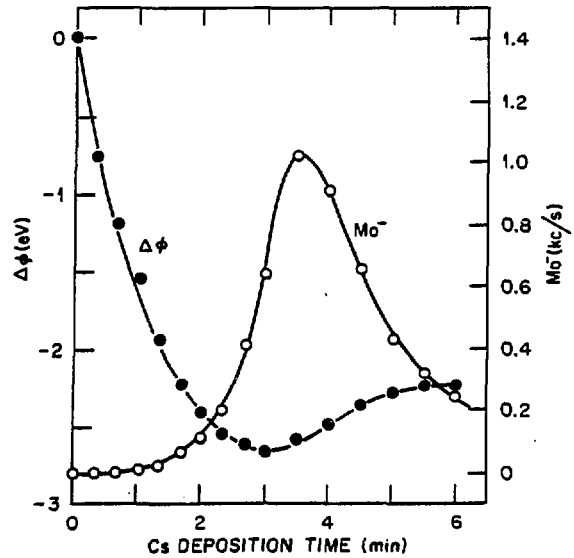

Fig. 13. Correlations between negative ion yield, surface work function change and cesium deposition time [Ref. 67].

Expression for the Negative Ion Current. A theoretical relationship between negative ion current I^- as a function of bombarding ion energy, E, responsible for sputtering the sample material, can be readily expressed using the appropriate surface ionization theoretical expression for computing the probability of ionization P_I, Sigmund sputtering theory for computing the sputtering ratio $S(E,\theta)$ [Ref. 70] and appropriate expression for the positive ion current (e.g., space charge limited analytical expressions where applicable). The negative ion so obtained current I^- is

$$I^-(E) = K(\theta_c)\, S(E,\theta)\, I^+(E)\, P_I\, P_{Ex} \qquad (4.2.1)$$

where P_{Ex} represents the probability that the particle will be extracted from the source once formed and $K(\theta_c)$ is a constant which takes into account the influence of the adsorbate if present on sputtering and particle ejection. $K(\theta_c)$ has values of $1 \rightarrow 0$. This expression does not take into account collisionally induced destructive processes which are current density or sputtered particle density dependent.

Quantum treatments of electron transfer processes which occur during interactions between atoms and metal surfaces or ions have been made by Sternberg [71] and Gadzuk [72]. A variety of metal-atom/ion interaction phenomena have been studied including resonance ionization of metastable atoms, resonance neutralization of ions, auger surface processes, negative ion formation and alkali metal adsorption. In such calculations, time dependent perturbation theory (or the equivalent first Born approximation) is used to predict transition probabilities of electrons to or from a metal and a bound atomic or free continuum state. Semiclassical transition probability theory has also been used to describe non-equilibrium processes for both positive and negative surface ionization [73,74].

The interaction of an atom with a metal at close distances results in a broadening and shifting of the valence or affinity levels of electropositive or electronegative atoms which enhances the probability of transfer of an

electron from the valence level to the Fermi sea or from the Fermi sea to the affinity level of the atom. The basic concepts underlying such processes were first suggested by Gurney in an early discussion of surface adsorption phenomena [75]. The theoretical bases for these mechanisms have been reviewed by Gadzuk [72].

Quantum mechanical treatment of the non-thermodynamic secondary ion emission problem has been treated by Nørskov and Lundqvist [76]. The model utilizes first order time dependent perturbation theory to calculate the probability that an initially occupied affinity level will survive during the non-adiabatic passage through and to an infinite distance from the surface. Away from adiabaticity there is a finite probability that the affinity level $|a\rangle$ will be occupied. During ejection the eigenenergy of $|a\rangle$, ε_a will vary with time or position due to interactions between the moving ion and substrate. In the model, the coupling between the substrate states $|k\rangle$ and the affinity level $|a\rangle$ is described by a hopping matrix $V_{ak}(t)$. The probability amplitude $a_{ak}(t)$ is then calculated by application of first order time dependent perturbation theory. The probability of occupancy at distances far from the metal are found to be exponentially dependent on $E_A - \phi$ and also dependent on the particle velocity v. Higher velocity particles in this model are ionized more efficiently than those with lower velocities. Experimental evidence supports this finding [73,74].

Quantum mechanical treatment of the scattering of low energy (100 eV) hydrogen ions with metal surfaces have also been made by Hiskes and Karo [77], and Hiskes, Karo and Gardner [78], and results commensurate with experimental negative ion formation probabilities from plasma type H^- sources based on the magnetron design concept were obtained [79]. Experimental investigation of H^- formation produced by back scattering H^+ ions from cesium covered surfaces have been investigated by Pargellis and Seidl [80]. The experimental results of Overbosch and Los [74] indicate that Na^- ions (~4%) can be relatively efficiently produced whenever 100 eV Na atoms are scattered from a hot single crystal tungsten surface partially covered with neutral sodium. The mechanism is considerably more efficient than those possible in conventional thermodynamic equilibrium surface ionization processes.

Information concerning the probability of negative ion formation during sputtering P_I is the most important aspect of the process needed to reliably predict negative ion yields. Unfortunately, the lack of a practically useful and generally applicable theoretical expression for calculating P_I has severely hampered correlation between experiment and theory. Despite several models which are presently in use, difficulties still exist in this area. In the following text, brief descriptions of selected models will be presented including the tunneling [81], the Nørskov and Lundqvist [76], the "freezing" approximation used by Overbosch and Los [73,74] and the modified surface ionization model [82,83]. These models have been discussed in more detail in an article by Alton [83].

The tunneling model. According to quantum theory, a free particle within a barrier of height V_0 of thickness a has a finite probability of escaping through the barrier even though its energy E is less than the barrier height V_0. The probability of escape from the barrier is simply the square of the ratios of the amplitudes of the incident and transmitted wave functions. The resulting probability of escape of an electron of energy E through the barrier for $0 < E < V_0$ is given by

$$P_I = \left\{\frac{1 + V_o^2 \sinh^2 \beta a}{1 + 4E(V_o - E)}\right\}^{-1} \qquad (4.2.2)$$

where

$$\beta = [2m(V_o - E)/h^2]^{1/2} \qquad (4.2.3)$$

for $\beta a \gg 1$

$$P_I \simeq \frac{16E(V_o - E)}{V_o^2} e^{-2\beta a} . \qquad (4.2.4)$$

In applications of the model to the sputtering problem, the electron is assumed to tunnel from the Fermi distribution within the solid through the barrier into the affinity level of the sputtered particle as it leaves the surface. Yu found that negative ion yield data generated by sputtering a molybdenum surface covered with Cs could readily be fitted by adjusting two parameters in the model, specifically the intrinsic work function ϕ_o and the barrier thickness a [67]. He further postulated that the cesium overlayer resulted in a reduction of the barrier height V_o by an amount $\Delta\phi$ and that $V_o - E = \phi_o + \Delta\phi$ where ϕ_o is the initial work function of the metal before cesium was added (the intrinsic work function). A schematic representation of the effect of an electropositive adsorbate on the surface barrier height is shown in Fig. 14. Since ϕ_o is identically equal to the intrinsic work function of the surface which is known for clean metals then one needs only to fit the data by adjusting a.

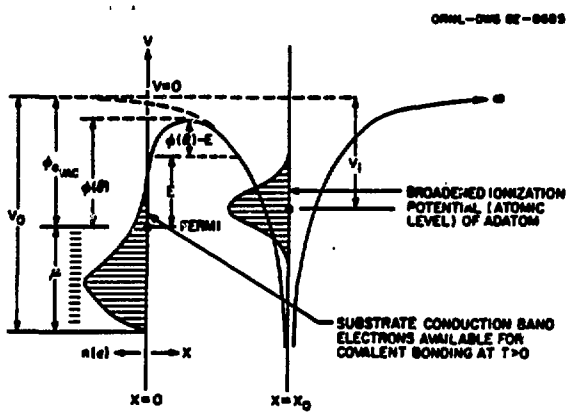

Fig. 14. Simplified potential energy diagram of a sputtered atom interacting with an electropositive adsorbate covered surface (tunneling theory).

The probability P_I then becomes

$$P_I \simeq \frac{16\, E_A(\phi_o + \Delta\phi)}{(\phi_o + \Delta\phi + E_A)^2} e^{-2\left(\frac{2m}{h^2}\right)^{1/2}(\phi_o + \Delta\phi)^{1/2}a} . \qquad (4.2.5)$$

We note that the expected exponential dependence on E_A does not appear in the model. Converse to expectation, the model predicts an inverse dependence on E_A which is very surprising and perhaps physically unrealistic. However, the tunneling model reproduces with surprising accuracy the experimental observations of Yu [67].

The Nørskov and Lundqvist model. The model of Nørskov and Lundqvist utilizes first order time dependent perturbation theory to calculate the probability that an initially occupied affinity level will survive during non-adiabatic passage of a particle through the surface [76]. A brief description of the model follows.

Away from adiabaticity, there is a finite probability that the affinity level $|a\rangle$, will be occupied. During ejection, the eigenenergy of $|a\rangle$, ε_a will vary with time or position due to interactions between the moving ion and the substrate. In the model, the coupling between the substrate states $|k\rangle$ and the affinity level $|a\rangle$ is described by a hopping matrix $V_{ak}(t)$. The derived differential probability is given by

$$dP_I = \frac{2}{\pi} e^{-\pi[C_1(\phi - E_A) + C_2]/h\gamma v}. \qquad (4.2.6)$$

In the previous expression ϕ is the work function of the metal and E_A is the value of the affinity far from the metal. We note that the model is energy dependent and requires two unknown parameters C_1 and C_2 in order to calculate negative ion formation probabilities. In order to correlate with experimental observation and thus determine P_I, one must integrate over the sputtered particle energy distribution function f(E) or

$$P_I = \frac{2}{\pi} \int_0^\infty f(E)\, e^{-\pi[C_1(\phi - E_A) + C_2]/h\gamma v}\, dE. \qquad (4.2.7)$$

The "freezing" approximation of Overbosch and Los. A semiclassical method has been used by Overbosch and Los for calculating the ionization probabilities of hyperthermal atoms scattered from metal surfaces [73,74]. The method is referred to as the "freezing" approximation since the electron transfer from the atom to the metal or from the metal to the atom is assumed to take place at a well defined position in space. The interaction between the scattered atom and metal is assumed to be binary — i.e. the atom interacts with a single atom of the metal which results in specular scattering from the surface. The incident and outgoing particle trajectories are approximated as straight lines in the model.

The probability of negative ionization from the metal surface is given by

$$P_I = \frac{1}{2} - \frac{1}{\pi} \arctan\left(\frac{E_A + \Delta E - \phi}{\Gamma/2}\right) \qquad (4.2.8)$$

where ΔE is given by the classical expression for the image charge

$$\Delta E_{\pm} = \pm \frac{e^2}{4z} \qquad (4.2.9)$$

and represents the shift in the valence or affinity level during interaction with the metal, E_A is the electron affinity, ϕ is the effective work function of the alkali metal covered surface, and Γ is the width of the affinity level near the surface. An illustration of this effect on the affinity level of an atom near a surface is exemplified in Fig. 15.

The modified surface ionization model. Although basic surface ionization theory is, in the strictest sense, only applicable to systems in thermodynamic equilibrium and the sputtering process does not meet this criterion, the results of the studies of Alton and Blazey [57] and Alton [82,83] using the modified University of Aarhus source, make what appears to be direct quantitative correlation with experiment using a modified surface ionization theory.

In this model, the probability of a particle leaving a surface as a negative ion is given by a modified form of the Langmuir-Saha relation

$$P_I = \frac{\frac{\omega^-}{\omega^0}\left[\frac{1-r^-}{1-r^0}\right] \exp\,(E_A-\phi)/kT}{1 + \frac{\omega^-}{\omega^0}\left[\frac{1-r^-}{1-r^0}\right] \exp\,(E_A-\phi)/kT} \qquad (4.2.10)$$

where r^-, r^0 are surface reflection coefficients for the negative, neutral particles, respectively, E_A is the atomic electron affinity of the target material at infinity, k is Boltzmann's constant, T is the effective temperature of the surface, ω^-, ω^0 are statistical weighting factors which are related to the total electronic spin of the respective species given by

$$\omega = 2\,\Sigma_i\, s_i + 1,$$

and ϕ is the value of the work function at optimum surface coverage. The effective temperature of the surface is found to be independent of source

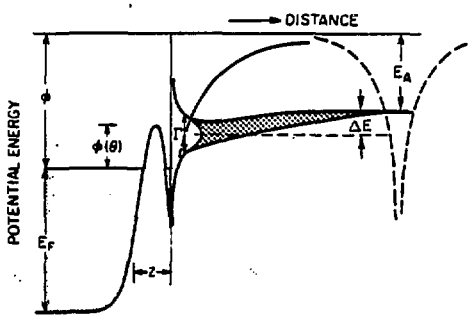

Fig. 15. Illustration of the shifting and broadening of affinity level of an atom near a metal surface.

operating conditions and assumed to be associated with the sputter process itself in the present application. This assumption is commensurate with the theoretical model of Nørskov and Lundqvist as well as recent experimental findings [76].

4.2.1 Types of Cesium Surface Ionization Sputter Sources

The Hortig-Mueller Source. Several versions of negative ion sources have evolved since the discovery by Krohn [65] that the negative ion yield of sputtered particles is greatly enhanced by the presence of a thin layer of cesium on the surface of the material being sputtered. The first of the sources was developed by Mueller and Hortig [84] and is illustrated by the schematic drawing shown in Fig. 16. The source consists of a continuously rotating wheel to which is attached an annular ring of the material to be sputtered. A thin layer of cesium metal is evaporated on the ring which is subjected to bombardment by approximately 20 keV positive argon ions which imping at an angle of 20° with respect to the surface. The negative ion yield produced in the sputtering process is then extracted by an electrode system. The source has produced a wide variety of negative ion beams including: 2.2 μA C^-; 0.4 μA MgO^-; 1 μA Cr^-; 6 μA Cu^-; 5 μA InO^-; 14 μA Ag^-; 4.6 μA TaO_2^-; 24 μA O^-; and 12 μA Au^-.

A source similiar in geometry has been developed by Alton which utilizes a cesium surface ionization source instead of the plasma source [85] and produces ion currents comparable to the Middleton-Adams source [68].

The Middleton Geometry Source. One of the most versatile of negative ion sources is the sputter source of Middleton and Adams [68]. A schematic drawing of the source illustrating the essential features is shown in Fig. 17. The source utilizes a cesium surface ionization source which is mounted at ground potential. A cesium beam of 0.1 to 1 mA is accelerated by a potential of ~20 kV and allowed to strike a conical surface of half angle approximately 20°. The cesium serves both as a sputtering agent and an electron donor in the formation of negative ions. The negative ions are extracted through an aperture in the apex end of the cone. The source is equipped with an externally indexable wheel containing several samples which permits rapid change of ion species. Gaseous material may also be introduced near the cone surface to enable formation of molecular negative ions and therefore extend the range of capability of the source. The versalitity of the ion source is exemplified

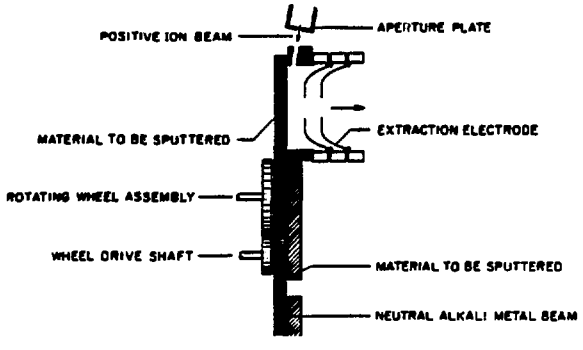

Fig. 16. Schematic drawing of the Mueller-Hortig negative sputter ion source [84].

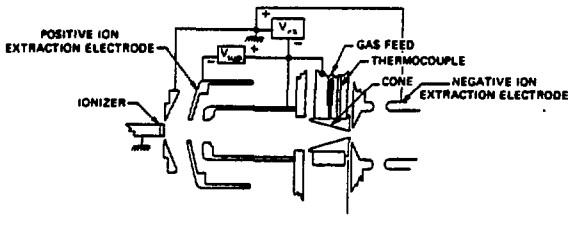

Fig. 17. Schematic drawing of the Middleton-Adams negative sputter ion source [68].

by the fact that the source has been used to produce ion beams containing most of the naturally occurring elements. Among the ion beams reported are: 20 μA H^-; 3 μA Li^-; 0.4 μA B^-; 40 μA C^-; 100 μA O^-; 30 μA F^-; 25 μA Si^-; 40 μA S^-; 4 μA P^-; 0.5 μA CaH_3^-; 0.8 μA Fe^-H; 10 μA Cu^-; 0.3 μA Bi^-; and 20 μA Au^-.

Several other versions of this source concept have been described in the literature including the sources of Alton [85], Doucas et al. [86], and the inverted sources of Chapman [87] and Yamanouchi et al. [88].

A version of the source which operates in the reflected beam mode has found practical use in sources of negative ions from very small isotopically enriched samples and as a concept useful in archeological dating experiments [89]. A schematic drawing of the negative ion generation region of this mode of operation is shown in Fig. 18.

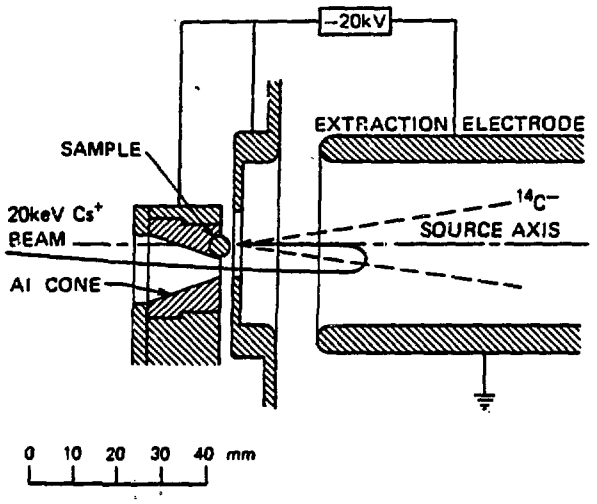

Fig. 18. Schematic drawing of the refocus-geometry Middleton-Adams source [Ref. 87] operated in the reflected beam mode.

Cesium Plasma Discharge Sources. Cesium rich plasma discharge sources, such as those developed at the University of Aarhus [69] and Oak Ridge National Laboratory [58] and the subsequently developed axial geometry counterparts [90-92] provide near optimum conditions for generation of negative ions by sputtering. Versions of the source developed at Oak Ridge National Laboratory [58,91] in the Aarhus and axial geometries are schematically illustrated in Figs. 19 and 20. The material of interest is mounted on a negatively biased probe and sputtered by cesium ions extracted from the plasma discharge. In addition to the energetic particles which sputter the sample, a neutral flux of cesium continuously strikes the surface. The ability to adequately provide and control the correct amount of surface cesium or other alkali metal during the sputtering process is of considerable importance for optimizing ion production from any source using this principle.

This particular source concept is to date the most prolific and among the most universal of sources having intensity capabilities of both atomic and molecular ion species which, in general, exceed other sources. These sources, as well, have lower emittances than those which utilize a positive ion beam to sputter the conical inner bore of a sample from which negative ions can be extracted. Among the ions and intensities which have been reported are the following: 175 μA H^-; 0.4 μA Li^-; 4 μA BeH_3^-; 25 μA BeO^-; 0.6 μA B^-; 20 μA C^-; 20 μA C_2^-; 30 μA O^-; 20 μA F^-; 12 μA S^-; 12 μA MgH_3^-; 20 μA Si^-; 20 μA F^-; 2.5 μA Al^-; 9 μA Al_2^-; 2 μA CaH_3^-; 2.5 μA TiH_3^-; 55 μA Ni^-; 50 μA Cu^-; ~1 μA SrH_3^-; 35 μA Ag^-; 3.1 μA TaN^-; 1.4 μA W^-; 80 μA Au^-; and 12 μA PbS^-.

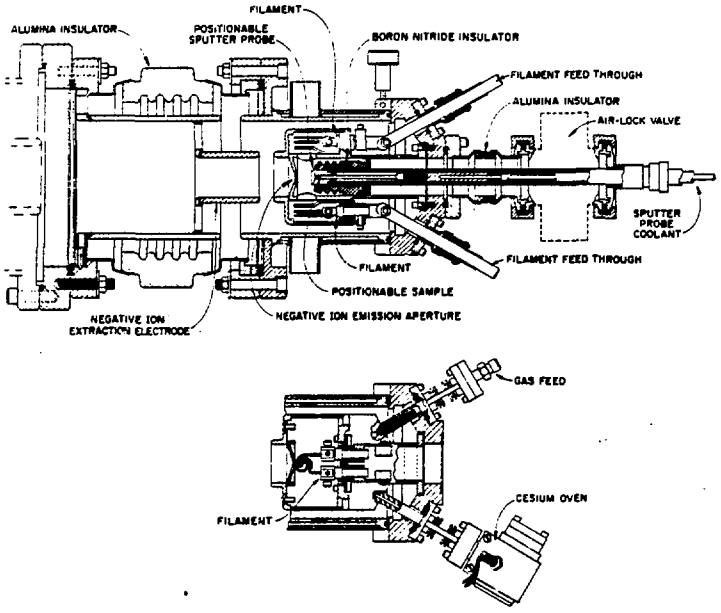

Fig. 19. Schematic drawing of the ORNL University of Aarhus geometry cesium-plasma negative ion sputter source [Ref. 57].

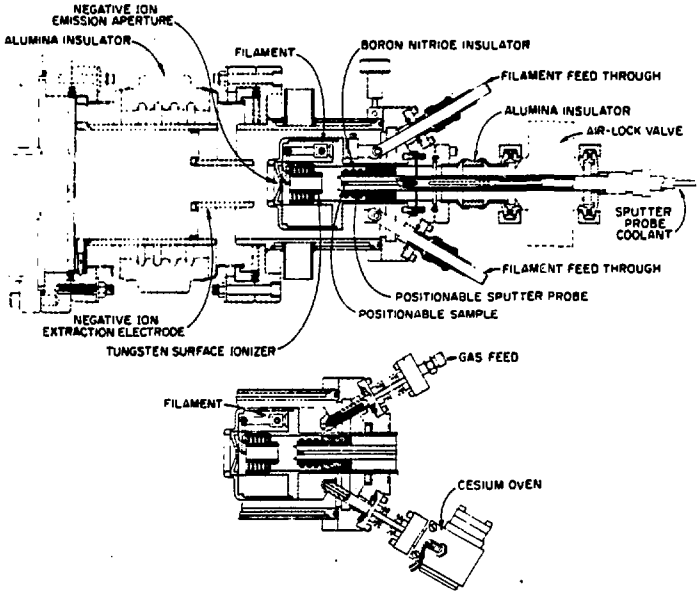

Fig. 20. Schematic drawing of the ORNL axial geometry cesium-plasma negative ion sputter source [Ref. 91].

A cold cathode Penning discharge version of the University of Aarhus cesium plasma source developed by Smith [93] is shown schematically in Fig. 21. The principal difference in the source concept is in the rather high discharge voltages (several hundred volts) required to maintain a stable

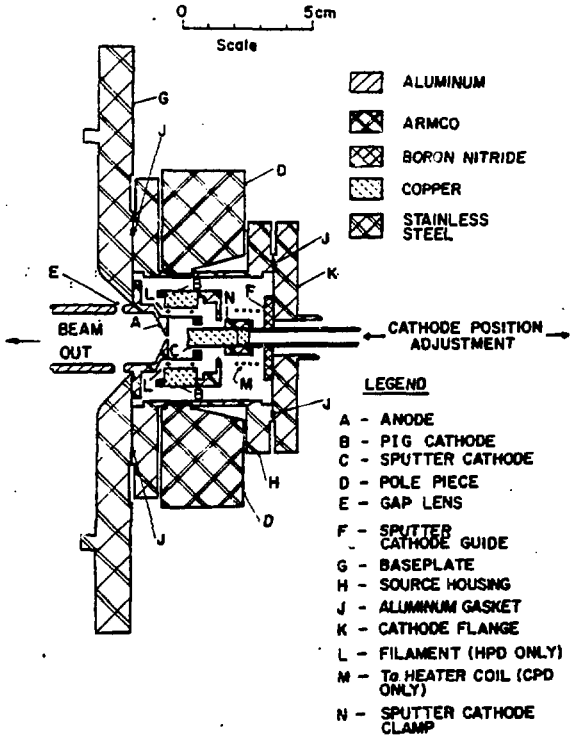

Fig. 21. Schematic drawing of the cold cathode University of Aarhus geometry negative ion sputter source of Smith [Ref. 93].

discharge. The source emittance for this configuration was found to be comparable to that measured for the hot cathode version of the source. Among the ion species and intensities reported are the following: 0.02 μA Li^-; 7μA C^-, 4 μA C_2^-; 0.14 μA Al^-; 1 μA Al_2^-; 0.8 μA U^-; 16 μA Ni^-; 8.4 μA Cu^-; 1 μA No^-; 0.14 μA Mo^-; and 1.2 μA Ta^-.

Other cesium plasma discharge type negative ion sources have been developed for H^- generation for possible use in neutral particle fusion research devices as well as other applications. These include the slit type Penning surface plasma source described by Allison [94] and further evaluated by Smith and Allison [95]. The source produces up to 80 mA of H^- when operated in cesium rich pulsed plasma mode.

The performance characteristics of several other negative H^- ion sources have been investigated for use in neutral particle injector-fusion energy research applications. All of the sources utilize Cs or a low work function cathode such as LaB_6 to produce H^- during surface ionization interactions. Among the sources described in the literature are the magnetron [79,96], the hollow cathode [97], the multicusp [98,99] and the multipole magnetic field bucket [100] sources.

5. Conclusions

Negative ion source technology has rapidly advanced during the past several years as a direct consequence of the discovery by Krohn [65] that negative ion yields can be greatly enhanced by sputtering in the presence of Group IA elements. Today, most negative ion sources use this discovery directly or the principles implied to effect negative ion formation through surface ionization. As a consequence, the more traditional direct extraction plasma and charge exchange sources are being used less frequently. However, the charge exchange generation mechanism appears to be as universal, is very competitive in terms of efficiency and has the advantage in terms of metastable ion formation.

In this review, an attempt has been made to briefly describe the principal processes involved in negative ion formation and sources which are representative of a particular principle. The reader is referred to the literature for specific details concerning the operational characteristics, emittances, brightnesses, species and intensity capabilities of particular sources.

References

*Supported by U.S.D.O.E., Division of Basic Energy Sciences with UCCND.

[1] K. H. Purser, R. B. Liebert, A. E. Litherland, R. P. Beukens, H. E. Gove, C. L. Bennett, M. R. Glover, and W. E. Sondheim, Rev. Phys. Appl. 12, 1487 (1977).

[2] K. Nishiizumi, J. R. Arnold, D. Elmore, R. Ferraro, H. E. Gove, R. C. Finkel, R. P. Beukens, K. H. Chang, and L. R. Kilius, Earth and Planetary Sci. Lett. 45, 235 (1979).

[3] J. M. Dawson, H. P. Furth, and F. H. Tenney, Phys. Rev. Lett. 26, 1156 (1971).

[4] H. P. Furth and D. L. Jassby, Phys. Rev. Lett. 32, 1176 (1974).

[5] B. R. Appleton, private communication.

[6] T. S. Noggle, B. R. Appleton, J. M. Williams, and O. S. Oen, Proceedings of the Fourth Conference on Applications of Small Accelerators, 76CH 1175-9 NPS (1976) 255.

[7] T. S. Noggle, B. R. Appleton, J. M. Williams, O. S. Oen, T. Iwata, G. W. Vogl (to be published).

[8] Y. Qiu, J. E. Griffith, W. J. Meng, and T. A. Tombrello, Radiation Effects 70, 231 (1983).

[9] B. R. Appleton, private communication.

[10] P. Williams and C. A. Evans, NBS Spec. Pub. 427, 63 (1975).

[11] S. Raman, to be published.

[12] C. A. Houser, I. S. Tsong, W. B. White, P. D. Miller, and C. D. Moak, Radiation Effects 64, 103 (1982).

[13] H. Hotop and W. C. Lineberger, J. Phys. Chem. Ref. Data 4, 539 (1975).

[14] L. M. Blau, R. Novick, and D. Weinflash, Phys. Rev. Lett. 24, 1268 (1970).

[15] R. Novick and D. Weinflash, Proc. Int. Conf. Precision Measurements and Fundamental Constants (Gaithersburg, MD 1970), eds. D. N. Langenberg and B. N. Taylor, Natural Bureau of Standards Spec. Publication No. 343, 403 (1971).

[16] J. Heinimier and P. Tykesson, Nucl. Instrum. and Meth. 141, 182 (1977).

[17] W. Kutschera and G. Korschinek, Proc. Sec. Int. Conf. on Ion Sources (Vienna Austria) (1972) 908.

[18] R. M. Dawton, IEEE Trans. Nucl. Sci. NS-19, No. 2, 231 (1972).

[19] R. Middleton, Nucl. Instrum. and Meth. 122, 35 (1974).

[20] G. D. Alton, Proc. Third Conf. on Applications of Small Accelerators, CONF-741040-P2 (1974) 11.

References (contd)

[21] G. D. Alton, "Ionization Phenomena and Sources of Ions," Chap. 2, Vol. 4 in Applied Atomic Collision Physics, edited by H. W. Massey et al. (Academic Press, Inc., New York), in press.

[22] H. W. Massey, "Negative Ions" Ch. 9, (Cambridge University Press, London, 1976).

[23] J. Franck, Trans. Faraday Soc. 21, 536 (1925).

[24] E. V. Condon, Phys. Rev. 32, 858 (1928).

[25] G. D. Alton, Nucl. Instrum. and Meth. 189, 15 (1981).

[26] M. Von Ardenne, Tabellen der Elektronenphysik, Ionenphysik und Übermikroskopie (VEB, Deutscher Verlag der Wissenschaften, Berlin, 1956).

[27] C. D. Moak, H. E. Banta, J. N. Thurston, J. W. Johnson, and R. F. King, Rev. Sci. Instr. 30, 694 (1959).

[28] A. P. Lawrence, R. K. Beauchamp, and J. L. McKibben, Nucl. Instrum. and Meth. 32, 357 (1965).

[29] M. Kobayashi, K. Prelec and Th. Sluyters, Rev. Sci. Instrum. 47, 1425 (1976).

[30] H. T. Richards and G. M. Klody, Proc. Sec. Int. Conf. on Ion Sources, Vienna (1972) 804.

[31] J. Aubert, G. Gautherin, and C. Lejeune, Proc. Sec. Int. Conf. on Ion Sources, Vienna (1972) 797.

[32] R. P. Bastide, N. B. Brooks, A. B. Wittkower, P. H. Rose, and K. H. Purser, IEEE Trans. Nucl. Sci. NS-12, 775 (1965).

[33] E. Heinicke, K. Bethge, and H. Bauman, Nucl. Instrum. and Meth. 58, 125 (1968).

[34] V. H. Smith and H. T. Richards, Bull. Am. Phys. Soc. 18 (1973).

[35] K. Prelec, Nucl. Instrum. and Meth. 144, 413 (1977).

[36] B. L. Donnally and G. Thoeming, Phys. Rev. 159, 87 (1967).

[37] G. I. Dimov and G. V. Roslyakov, Instr. Expl. Tech. 17, 658 (1974).

[38] R. J. Girnius, C. J. Anderson, and L. W. Anderson, Phys. Rev. A 16, 2225 (1977).

[39] B. A. D'Yachkov and V. I. Zinenko, Sov. Phys. — Tech. Phys. 16, 305 (1971).

[40] R. M. Ennis, Jr., D. E. Schechter, G. Thoeming, D. B. Schlafke, and B. L. Donnally, IEEE Trans. Nucl. Sci. NS-14, 75 (1967).

References (contd)

[41] R. J. Girnius and L. W. Anderson, Nucl. Instrum. and Meth. 137, 373 (1976).

[42] A. S. Schlacter, D. H. Loyd, P. J. Bjorkholm, L. W. Anderson, and W. Haeberli, Phys. Rev. 174, 201 (1968).

[43] J. Heinemeier and P. Hvelplund, Nucl. Instrum. and Meth. 148, 65 (1975).

[44] J. Heinemeier and P. Hvelplund, Nucl. Instrum. and Meth. 148, 425 (1975).

[45] W. Gentner and G. Hortig, Z. Phys. 172, 357 (1963).

[46] G. F. Wells and G. D. Alton, unpublished.

[47] E. B. Hooper, Jr., P. A. Pincosy, P. Poulsen, C. F. Burrell, L. R. Grisham, and D. E. Post, Rev. Sci. Instrum. 51, 1066 (1980).

[48] G. D. Alton, to be published.

[49] T.J.L. Greenway, Oxford University Report 85/77 (1977).

[50] J. B. Taylor and I. Langmuir, Phys. Rev. 44, 423 (1933).

[51] J. A. Becker, Trans. Faraday Soc. 28, 151 (1932).

[52] R. L. Gerlach and T. N. Rhodin, Surface Science 17, 32 (1969).

[53] D. L. Fehrs and R. E. Stickney, Surface Science 24, 309 (1971).

[54] M. Blaszczyszyn, Surface Sci. 59, 533 (1976).

[55] A. R. Miller, Proc. Cambridge Phil. Soc. 42, 292 (1946).

[56] J. J. Broeder, L. L. van Reijen, W.M.H. Satchler, and G.C.A. Schuit, Z. Electrochem 60, 838 (1956).

[57] G. D. Alton and G. C. Blazey, Nucl. Instrum. and Meth. 166, 105 (1979).

[58] N. D. Lang, Phys. Rev. B 4, 4234 (1971).

[59] M. Kaminsky, Atomic and Ionic Impact Phenomena on Metal Surfaces (Springer Verlag, New York, 1965).

[60] R. N. Compton, P. W. Reinhardt, and W. R. Garrett, J. Chem. Phys. 66, 4712 (1977).

[61] G. D. Alton, unpublished.

[62] P. F. Dittner and S. Datz, J. Chem. Phys. 68, 2451 (1978).

[63] G. D. Alton, unpublished.

References (contd)

[64] N. Kashihira, E. Vietzke, and G. Zellermann, Rev. Sci. Instrum. 48, 171 (1977).

[65] V. E. Krohn, Jr., Appl. Phys. 33, 3523 (1962).

[66] M. K. Abdullayeva, A. K. Ayukhanov and V. G. Shamsiyev, Determination of the Negative Ion Yield of Copper Sputtered by Cesium Ions in Ion Surface Interactions, Sputtering and Related Phenomena, eds. R. Behrish, W. Hieland, W. Poschanvieder, P. Staib, and H. Verbeek (Gordon Breach, London, 1973).

[67] M. L. Yu, Phys. Rev. Lett. 40, 574 (1978).

[68] R. Middleton and C. T. Adams, Nucl. Instrum. and Meth. 118, 329 (1976).

[69] H. H. Andersen and P. Tykesson, IEEE Trans. Nucl. Sci. NS-22, 1632 (1975).

[70] P. Sigmund, Phys. Rev. 184, 383 (1969).

[71] D. Sternberg, Ph.D. Dissertation, Dept. of Physics, Columbia University (1957).

[72] J. W. Gadzuk, Surface Sci. 6, 133 (1967).

[73] E. G. Overbosch and J. Los, Surface Sci. 108, 59 (1981).

[74] E. G. Overbosch and J. Los, Surface Sci. 108, 117 (1981).

[75] R. W. Gurney, Phys. Rev. 47, 479 (1935).

[76] J. K. Nørskov and B. I. Lundqvist, Phys. Rev. B 19, 5661 (1979).

[77] J. R. Hiskes and A. Karo, Proc. Symp. on the Prod. and Neutralization of Negative Hydrogen Ions and Beams (Brookhaven National Laboratory, 1977) 42.

[78] J. R. Hiskes, A. Karo, and M. Gardner, J. Appl. Phys. 47, 3888 (1976).

[79] Yu. I. Belchenko, G. I. Dimov, and V. G. Dudnikov, Proc. Sec. Symp. on Ion Sources and Formation of Ion Beams (Berkeley, CA 1974), VIII-1, LBL-3399 (1974).

[80] A. Pargellis and M. Seidl, Phys. Rev. B 25, 4356 (1982); M. Seidl and A. Pargellis, Phys. Rev. B 26, 1 (1982).

[81] L. I. Schiff, Quantum Mechanics, (McGraw-Hill, New York, 1968), Third Edition.

[82] G. D. Alton, Proc. Third Int. Conf. on Electrostatic Accel. Tech. (Oak Ridge, TN, 1981) 228.

[83] G. D. Alton, IEEE Trans. Nucl. Sci. NS-30, No. 2, 1480 (1983).

References (contd)

[84] M. Mueller and G. Hortig, IEEE Trans. Nucl. Sci. NS-16, 38 (1969).

[85] G. D. Alton, IEEE Trans. Nucl. Sci. NS-23, 1113 (1976).

[86] G. Doucas, H. R. McK. Hyder, and A. B. Knox, Oxford Univ. Report (1975).

[87] K. R. Chapman, IEEE Trans. Nucl. Sci. NS-23, No. 2, 1109 (1976).

[88] M. Yamanouchi, Y. Higashi, H. Yamaguchi, and M. Okamoto, Nucl. Insrum. and Meth. 158, 339 (1979).

[89] K. Brand, Nucl. Instrum. and Meth. 154, 595 (1978).

[90] G. T. Caskey, R. A. Douglas, H. T. Richards, and H. V. Smith, Jr., Nucl. Instrum. and Meth. 157, 1 (1978).

[91] G. D. Alton, IEEE Trans. Nucl. Sci. NS-26, 3708 (1979).

[92] R. Middleton, Proceedings of Northeastern Symposium for Accelerator Personnel, University of Wisconsin, Oct. 13-15, 1980), p. 134.

[93] H. V. Smith, Nucl. Instrum. and Meth. 164, 1 (1979).

[94] P. W. Allison, IEEE Trans. Nucl. Sci., NS-24, 1594 (1977).

[95] H. V. Smith and P. Allison, Rev. Sci. Instrum. 53, 405 (1982).

[96] J. G. Alessi and Th. Sluyters, Rev. Sci. Instrum. 51, 1630 (1980).

[97] M. Kobayashi, K. Prelec and Th. Sluyters, Rev. Sci. Instrum. 47, 1425 (1976).

[98] K. N. Leung and K. W. Ehlers, Rev. Sci. Instrum. 53, 803 (1982).

[99] K. N. Leung, K. W. Ehlers, and M. Bacal, Rev. Sci. Instrum. 54, 56 (1983).

[100] F. Sano, T. Obiki, A. Sasaki, A. Iiyoshi, and K. Uo, Rev. Sci. Instrum. 54, 41 (1983).